ELSEVIER

Journal of South American Earth Sciences 19 (2005) 111–125

Journal of
South American
Earth Sciences

www.elsevier.com/locate/jsames

Geometric and kinematic model for basement-involved backthrusting at Diamante River, southern Andes, Mendoza province, Argentina

M.M. Turienzo[a,b,*], L.V. Dimieri[a,b]

[a]*Departamento de Geología, Universidad Nacional del Sur, San Juan 670, S8000 Bahía Blanca, Argentina*
[b]*Consejo Nacional de Investigaciones Científicas y Técnicas, Rivadavia 1917, 1033 Buenos Aires, Argentina*

Received 1 November 2003; accepted 1 December 2004

Abstract

At the confluence of the Las Aucas stream with the Diamante River (69°30′W Long.; 34°40′S Lat.), kilometer-scale structures affecting basement rocks were surveyed. Andean deformation involved both Cordillera Principal and Cordillera Frontal rocks, whose structures probably were locally contemporaneous and intimately related. The Cordón del Carrizalito, a huge structure interpreted as a rigid basement block raised by a reverse fault on the eastern edge, which produced intense deformation in the sedimentary cover, can be explained by a geometric and kinematic model for basement-involved structures in the upper crustal levels. The Lomas Bayas structure is considered a west-vergent anticline associated with a backthrust, which branches out from the basement block's eastern edge. A new kinematic quantitative model, based on the Lomas Bayas structure, explains basement-involved backthrusts. Shearing of the basement rocks produced progressive rotation of the backthrust's hangingwall block, whose upper toe is bent but sedimentary cover is delaminated and detached. These retrodeformable models are applied to two cross-sections to test their viability and calculate the structural shortening.

Keywords: Backthrusts; Basement tectonics; Kinematic model; Southern Andes

Resumen

En la confluencia del arroyo Las Aucas y el Río Diamante (69°30′ LO; 34°40′ LS) se observan estructuras de escala kilométrica afectando al basamento. La deformación andina en este sector involucra a las rocas de la Cordillera Principal y de la Cordillera Frontal, cuyas estructuraciones serían localmente contemporáneas y relacionadas. El Cordón del Carrizalito constituye una gran estructura que consideramos como un bloque rígido de basamento, elevado mediante una falla inversa ubicada en su borde oriental, que deforma intensamente la cubierta sedimentaria. Para explicar su desarrollo se utilizó un modelo geométrico y cinemático para estructuras que afectan al basamento en condiciones superficiales. La estructura de Lomas Bayas es considerada un anticlinal con vergencia hacia el oeste asociado a un retrocorrimiento que se desprende del extremo oriental del bloque de basamento elevado. Basados en esta estructura, elaboramos un nuevo modelo cinemático cuantitativo para la formación de retrocorrimientos que involucran al basamento. Debido al cizallamiento en las rocas del basamento, el bloque encima del retrocorrimiento rota progresivamente y su extremo flexionado produce delaminación y despegue de la cubierta sedimentaria. Estos modelos aplicados a dos secciones transversales permitieron calcular los acortamientos y sus variaciones a lo largo del rumbo.

Palabras clave: Retrocorrimientos; Tectónica de basemento; Modelo cinemático; Andes del Sur.

1. Introduction

The studied region includes the Lomas Bayas area and the western sector of the confluence of the Diamante River with the Las Aucas stream, which is located in the central western portion of the Mendoza province (69°30′W; 34°40′S), approximately 100 km north of Malargüe City (Fig. 1a).

* Corresponding author. Address: Departamento de Geología, Universidad Nacional del Sur, San Juan 670, S8000 Bahía Blanca, Argentina. Tel.: +54 291 4595101; fax: +54 291 4595148.
E-mail addresses: turienzo@uns.edu.ar (M.M. Turienzo), ghdimier@criba.edu.ar (L.V. Dimieri).

0895-9811/$ - see front matter © 2005 Elsevier Ltd. All rights reserved.
doi:10.1016/j.jsames.2004.12.002

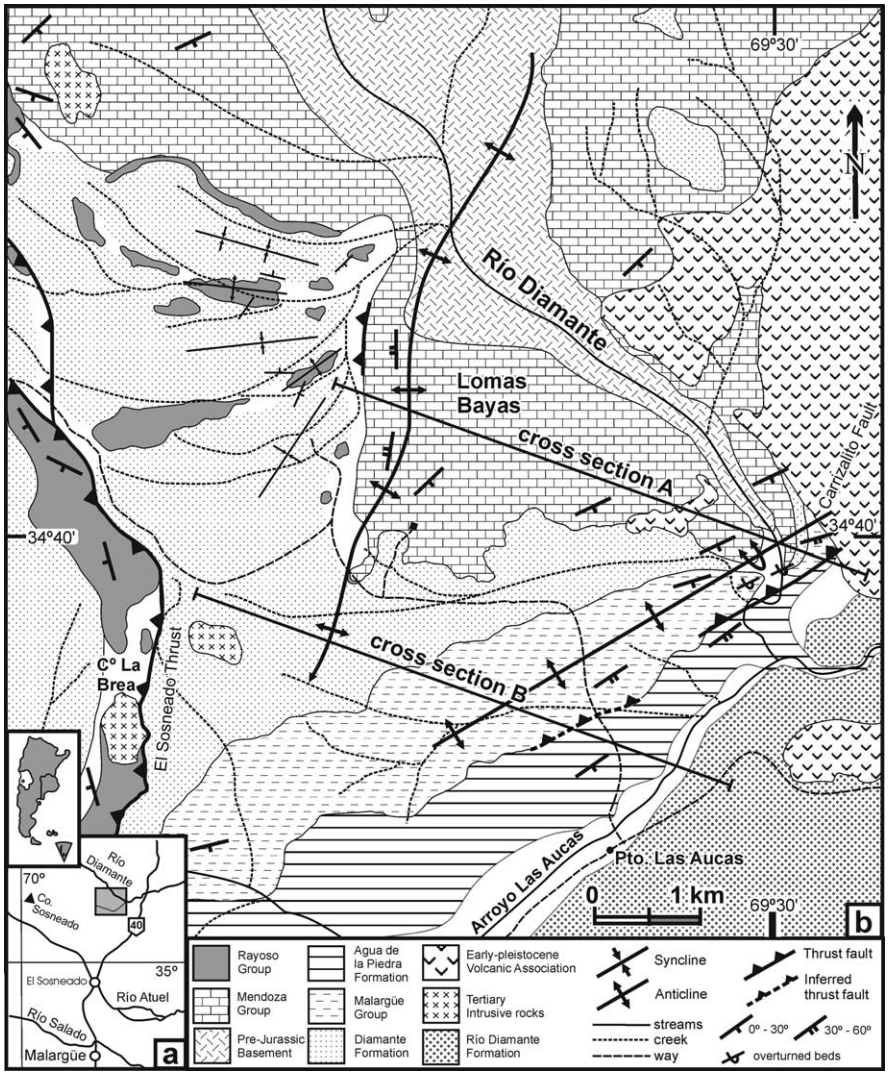

Fig. 1. (a) Location of the studied area. (b) Structural and geologic map from the Diamante River/Las Aucas stream confluence area, west of Mendoza province. Note the location of cross-sections A and B.

The surveyed area involves two geological provinces—the Cordillera Principal and Cordillera Frontal—whose boundaries follow the Diamante River valley. The former is represented by the Malargüe fold-and-thrust belt (Kozlowski et al., 1993) and the latter by the Cordón del Carrizalito, which is composed of Paleozoic to Permian-Triassic metamorphic and igneous rocks. The distinction between these geological provinces is based mainly on geographic, topographic, and stratigraphic criteria. In the past century, some geologists have noted the tectonic influence of the Cordillera Frontal basement rocks on the Cenozoic and Mesozoic cover materials of the Cordillera Principal (e.g. Ghert, 1931; Groeber, 1947; Polanski, 1962, 1963). We agree with these early researchers that these geological provinces are structurally linked according to the way in which the Andean orogeny affects them. Modern regional geological surveys have been provided by Volkheimer (1978; Cerro Sosneado) and Sruoga et al. (2002; Volcán Maipo), but there are few detailed structural works that pertain to this area (Baldi et al., 1984; Kozlowski, 1984; Kozlowski et al., 1993; Nullo and Stephens, 1993; Manceda and Figueroa, 1995; Fortunatti and Dimieri, 1999; 2002; Giambiagi et al., 2001; Giambiagi and Ramos, 2002; Ramos, 2002; Fortunatti et al., 2004; Turienzo et al., 2004).

The southern edge of the Cordillera Frontal, locally composed of the Cordón del Carrizalito, is a large basement block uplifted by moderately to steeply dipping reverse faults that protrude and deform the sedimentary cover intensely. Although different geometrical and kinematical models have been proposed to link the deformation of rigid basement blocks and sedimentary cover (e.g. Erslev, 1991; Erslev and Rogers, 1993; McConnell and Wilson, 1993; Narr and Suppe, 1994; Mitra and Mount, 1998; Allmendinger, 1998), to reconstruct the Cordón del Carrizalito structure, we follow the techniques developed by Narr and Suppe (1994) for basement-involved compressive structures in a fragile domain. This reconstruction provides a reasonable explanation of the evolution

and configuration of the structures in the study area, though we note that other models can be used to reconstruct the structural features observed.

The structure that forms Lomas Bayas is interpreted as a minor anticline associated with a backthrust that affected the eastern edge of the uplifted basement block. However, most models explain only the geometry and kinematics of larger structures, not the smaller ones associated with them, and classic kinematic models of backthrust development cannot reproduce the shape of the Lomas Bayas structure. In this article, we propose a viable interpretation of the major and minor structures that outcrop in the study area and introduce a new kinematic model to explain backthrust generation associated with an uplifted basement block. The backthrust hangingwall is a wedge-shaped basement block that rotates progressively because of shearing in the footwall rocks. We elaborate a quantitative diagram in which we establish the geometric relationship between the wedge rotation angles and the required angular shear. Finally, we use the model to explain the geometry of the Lomas Bayas structure and calculate the tectonic shortening and changes along-strike on two retrodeformable cross-sections.

2. Geological setting

As we mentioned previously, the studied zone comprises the boundary between the Cordillera Frontal and Cordillera Principal, which show distinct geological features. Outcrops in this region present several lithologic types, mainly Paleozoic-Quaternary igneous, sedimentary, and metamorphic rocks (Fig. 1b), which makes the area significant for studying the evolution of both geological provinces. For a better understanding of the stratigraphy, we briefly describe the different units and the structures that affect them. (For more detailed information about the lithological characteristics of the stratigraphic units, see Groeber, 1947; Volkheimer, 1978; Sruoga et al., 2002.) The thicknesses of each unit in the cross-sections represent averages of values taken from previous work and our field data.

2.1. Stratigraphy

2.1.1. Pre-Jurassic basement

The unit is composed of sedimentary and low-grade metamorphic rocks of the Las Lagunitas Formation (Devonian), intruded by the Carrizalito tonalite (Carboniferous). This igneous–metamorphic assemblage was intruded by Permian-Triassic granitic rocks and covered by basaltic-rhyolitic volcanic and phyroclastic rocks assigned to the Choiyoi cycle (Llambias et al., 1993). On the basis of its lithologic composition and rheologic behavior, some researchers have questioned whether it can be considered a crystalline basement (Gorroño et al., 1984; Kozlowski, 1984; Dimieri, 1992; Dimieri and Nullo, 1993). We suggest that this unit acts like a rigid element, given that, locally, intrusive materials represent it almost exclusively (Fig. 2).

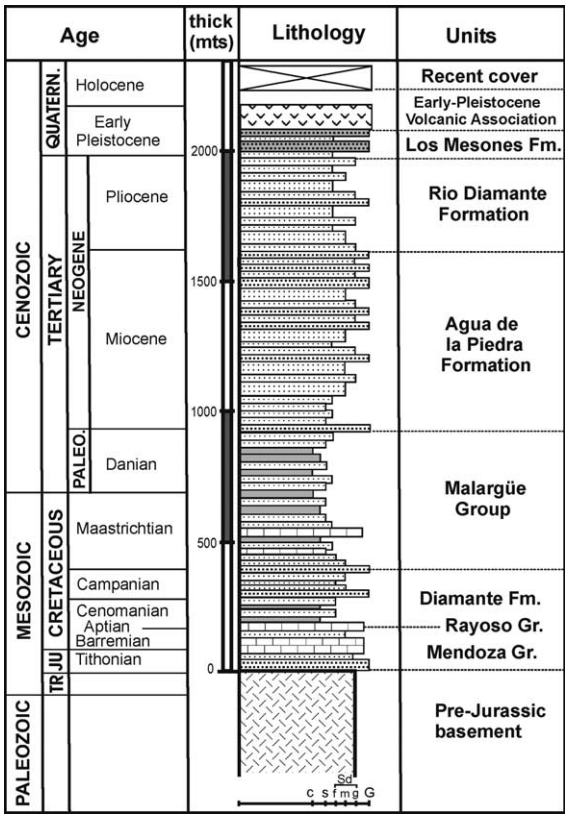

Fig. 2. Schematic stratigraphic column of the units with age, thickness, and lithology.

2.1.2. Mendoza group (Tithonian–Barremian)

This unit presents a marked transgressive character in the Diamante River area, with proximal facies unconformably covering pre-Jurassic rocks. In Lomas Bayas, a thick basal conglomerate grades to yellowish, calcareous, partly coarse-grained sandstones. Fossiliferous calcareous beds dominate the upper section. The sequence corresponds to the Vaca Muerta, Chachao, and Agrio Formations (Sruoga et al., 2002) and could indicate transitional conditions between continental and marginal marine environments. According to Volkheimer (1978), the whole thickness is approximately 155 m.

2.1.3. Rayoso group (Aptian–Cenomanian)

This group has been divided in two units: the Huitrin Formation, composed of evaporites and calcareous rocks, and the Rayoso Formation, composed mainly of red terrigenous facies of siltstones and sandstones (Sruoga et al., 2002). In the study area, a thick, grayish, calcareous bed with marked internal lamination occurs, and no fossiliferous content other than some algal structures is noticeable. Small-scale tectonic structures and repetitions in the westernmost region are common, as is gentle folding west of Lomas Bayas (Fig. 1b). This bed could be assigned

to a carbonate member of the Huitrin Formation. The rocks of the group may indicate alternation between hypersaline marine and continental, fluvial to mud plain environments (Sruoga et al., 2002). We use an average thickness of 50 m.

2.1.4. Diamante formation (Neocenomanian–Campanian)

The unit is composed of reddish clastic rocks, included in the Diamantiano cycle by Groeber (1946) and named the Salas Formation by Volkheimer (1978). The rocks are mainly red sandstones and conglomerates with abundant sedimentary structures and could be correlated partially with the Neuquén Group (Bettini et al., 1978; Legarreta and Gulisano, 1989). Moreover, a conglomeratic bed, extended and continuous along the Malargüe Group's contact and dipping 30°SE, stands out (Fig. 3). The thickness of this unit at the Diamante River area ranges from 100 to 250 m; it was formed by alluvial fans and braided systems of proximal facies of the basin (Cruz, 1993).

2.1.5. Malargüe group (Maastrichtian–Danian)

This sequence has been divided by Legarreta and Gulisano (1989) into four formations. One section includes the Las Aucas stream (Volkheimer, 1978), where the sequence seems complete. The base of the Loncoche Formation is composed of conglomerates and coarse-grained sandstones that turn into thin-grained materials. The conglomeratic bed in contact with the younger Diamante Formation could belong to the latter. Limestones, siltstones, and calcareous sandstones with abundant fossil content compose the Roca Formation. Fine-grained clastic sediments compose the Pircala and Coihueco Formations, which are characterized by their pale green color (Sruoga et al., 2002). The sequence is thicker than 500 m at Las Aucas stream, though it may reduce nearer the highlands. Sudden bed thinning near the Diamante River could be a tectonic phenomenon.

2.1.6. Agua de la Piedra formation (Middle Miocene)

Composed of an upward-coarsening grain sequence with tuffaceous reddish sandstones at its base, this unit grades to conglomeratic facies with predominant andesitic pebbles near the top. A conglomeratic level known as 'rodados lustrosos' (Groeber, 1946) serves as the base in most sections, which may correspond to an alluvial fan environment linked to the Andean uplift (Combina et al., 1994). Thicknesses are highly variable, though we estimate an average of 700 m (Kozloswki and Baldi, 1983).

2.1.7. Río Diamante formation (Pliocene)

Pale red and conglomeratic sandstones with volcanic material lie unconformably over the Agua de la Piedra Formation and are interpreted as alluvial fans in the distal sections of braided fluvial systems (Combina et al., 1993). A subhorizontal thick sequence of approximately 110 m, south of the Las Aucas stream, was reported by Combina et al. (1993), though the base is not visible. Nearby, it may reach 500 m thick (Kozloswki and Baldi, 1983).

We also must highlight the presence of the Andesita La Brea subvolcanic bodies (Nullo et al., 2002), which intrude the Mesozoic sequences and belong to the Huincán eruptive cycle (Miocene). Important coarse agglomerate levels compose the Los Mesones Formation (Lower Pleistocene) and are considered alluvial fan systems linked to the uplifting of the mountain front (Polanski, 1963). Finally, extended volcanism, represented by basaltic and andesitic flows and locally ignimbritic levels, also developed and was defined by Polanski (1963) as the Early Pleistocene volcanic association.

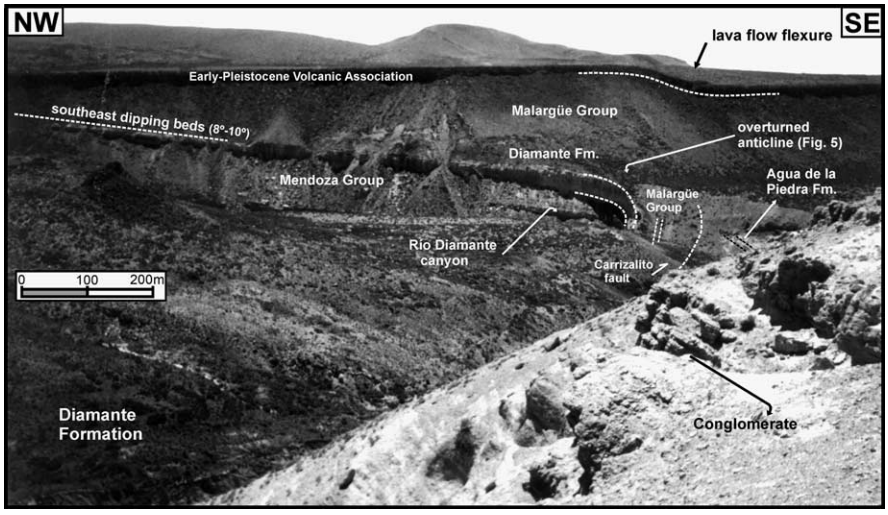

Fig. 3. Panoramic view of the structure located in the north wall of the Diamante River canyon. Note the southeastern slightly dipping beds and anticline structure with thinned layers related to the Carrizalito fault, as well as the basaltic flow flexure just above the structure. At the front, a conglomeratic level lies between the Diamante Formation and Malargüe Group.

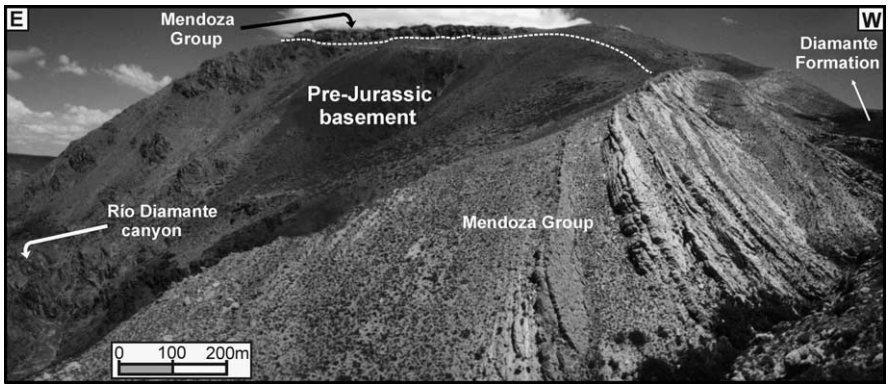

Fig. 4. Oblique photo of the Lomas Bayas anticline, generated by a backthrust-related basement wedge.

2.2. Structure

The Lomas Bayas structure is a pre-Jurassic, basement-cored, asymmetric anticline vergent to the hinterland (Fig. 4). The forelimb has an almost constant dip of 35°W, whereas the backlimb gently dips SE at angles of 12–6°. In a small area near the fold hinge, the backlimb has a flexure that reaches 20° dip. For simplicity in our geometric reconstruction, we use a 10° average value, equivalent to the uniform dip of the same layers at the north side of the Diamante River valley (Fig. 3). To the east, following the Las Aucas stream, the strata become gradually steeper, as can be observed at the contact of the Diamante Formation with the Malargüe Group, where a conglomeratic bed dips approximately 30°SE (Fig. 3). Overlying Tertiary units assigned to the Río Diamante Formation are steeper and reach up to 60°. At the northern margin of the Diamante River, near its confluence with the Las Aucas stream, the top of the basement is exposed and, with the cover sedimentary rocks, forms a SE-vergent drape fold (Fig. 5). The eastern limb of this anticline steeply dips to overturned and very thin. The Carrizalito fault is located immediately east of Mesozoic beds that are overthrust above Tertiary rocks. Cenozoic layers become horizontal farther east. The depth of the basement–cover interface in the footwall area was taken from Baldi et al. (1984). Lava flows that crown the north side of the Diamante River are slightly bent just above the Carrizalito fault trace (Fig. 3), which has been interpreted as triggered by Quaternary tectonic activity that reactivated the fault (Kozloswki, 1984).

In addition, several structures have been mapped elsewhere in the study area (Fig. 1b) but not included in the models; thus, we describe them briefly. In the western region, a fault—the El Sosneado thrust (Nullo et al., 1987)—repeats calcareous beds of the Rayoso Group and places them over the reddish beds of the Diamante Formation. At the easternmost sector of the studied area, minor thrust-related anticlines and synclines, partially mapped by Nullo and Stephens (1993), involve the Rayoso Group and Diamante Formation, have a NE–SW to E–W trend, and form part of a synclinorium west of Lomas Bayas. This gentle folding may be accommodation structures related to basement uplifts or have existed prior to the basement structuring; its origin remains unclear. The structures are connected to the west side of the Lomas Bayas anticline, where distinguishing among the boundaries of the units is not possible because of the poorly exposed outcrops. However, evidence of faulting that affected the Mendoza Group limestones is apparent and has been interpreted as splays of the Sosneado thrust that were folded by younger, basement-involved faults located at the eastern footwall (Kozloswki et al., 1989; Nullo and Stephens, 1993).

3. Previous interpretations

In the eastern sector of Cordillera Frontal, Ghert (1931) distinguished first-order, basement-cored, primary or deep folding characterized by a wide vault arch. The author assigned the Moradito anticline to this structure, according to the old denomination of the hills now known as Cordón del Carrizalito. According to Ghert (1931), the first-order structures are large, and the basement is involved in

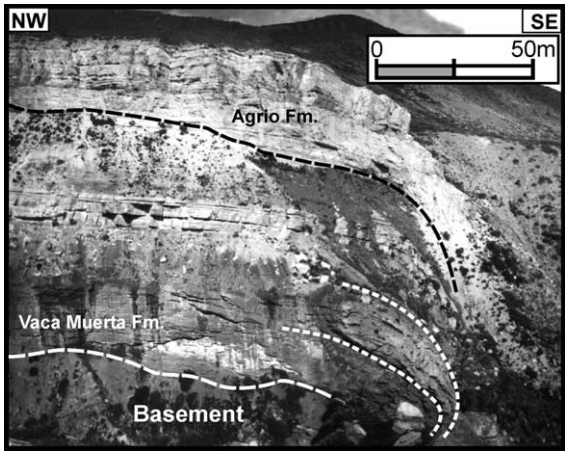

Fig. 5. Detail of the anticline structure related to the Carrizalito fault, north side of Diamante River. Eastern limb beds are markedly thinned and subvertical.

the deformation. However, second-order structures correspond to a set of smaller thrusts and folds that detach from the basement, generally along evaporite layers of the covering sedimentary sequence. For the structural analysis presented herein, we use the term 'major' for those structures that produce the largest shortening and/or imply large fault slips; the Carrizalito fault affecting the basement represents the major structure. Conversely, we use 'minor' or 'subsidiary' structures to refer to those that imply small shortening and/or slipping and are genetically linked to the major structures, with or without the participation of basement rocks in the deformation. According to Groeber (1938), the Cordillera Frontal uplift, 'in mass or blocks,' was achieved by a reverse fault system at the eastern border. Through this faulting, the Cordillera Frontal 'has been slightly overthrusted and it has advanced some distance above the longitudinal depressions of Uspallata and Tunuyán valleys' (Groeber, 1938). Although regional, this point of view shows that the author studied a deformation of faulted, foreland-directed basement blocks that overthrust Tertiary basins. According to Polanski (1962, 1963), the uplift of the Cordillera Frontal appears like a big arch that involved the Cordillera Principal structures, and these geological provinces acted as tectonically tied units.

Complex cover deformation linked to important basement block uplifting, which is gently folded and limited by steeply faults, has been noted by Baldi et al. (1984) and Kozloswki (1984). Folded layers related to these faults have steep to overturned dips and undergo thinning and extensional faulting, which omits strata. These authors believe that cover rocks in the Diamante River area are proximal facies that behave rigidly and deform together with the basement; thus, both basement and cover shortening are equivalent (Baldi et al., 1984). According to Kozloswki (1984), the Cordón del Carrizalito forms a large, asymmetric anticline with a 30° dipping western limb and a subvertical east limb limited by a high-angle fault that reaches the surface near the Las Aucas stream/Diamante River confluence. This fault was readily recognized by Lahee (1927), who named it the Diamante fault. The southward-plunging Cordillera Frontal could be related to a decreasing slip south of the Diamante fault (also known as the Carrizalito fault; Kozloswki et al., 1989). Kozloswki (1984) interprets the Lomas Bayas structure as a minor fault-related anticline without detachments between the basement and the cover. The Lomas Bayas structure also has been considered an anticline related to an east-dipping fault (Kozlowski et al., 1993).

Other structural interpretations of the mountain front between the Diamante and Salado Rivers support basement deformation by both fault propagation and fault-bend folds, which generated foreland-vergent structures with steep to overturned frontal limbs (Kozlowski et al., 1993; Manceda and Figueroa, 1995). Nullo and Stephens (1993) propose that, in this region, the Carrizalito fault raised the Cordillera Frontal block after 5 Ma, while an antithetic fault system deformed the sedimentary sequence at the western margin of the studied region. Furthermore, sedimentary beds at Lomas Bayas may have undergone accommodation above a subvertical fault that affected the basement. These authors interpret the Cordón del Carrizalito structure as a discontinuous anticlinorium, and its culmination could be marked by the NE-SW-trending normal Las Aucas fault. Recent studies performed in northern sectors indicate that the Cordillera Frontal uplift is related to the eastward migration of the thrust front between 8.5 and 6 Ma (Giambiagi and Ramos, 2002). This uplift evolved at different times from north to south and thus could have been active after 6 Ma in the southern areas (Giambiagi et al., 2001).

4. Backthrust development model

Important backthrust systems, continuous along-strike, have been described in several places in the Malargüe fold-and-thrust belt. At Bardas Blancas, 50 km south of Malargüe City (Fig. 1a), backthrusts form an imbricated wedge system that involves basement rocks of the Choiyoi cycle (Dimieri, 1992, 1997; Dimieri and Nullo, 1993). Backthrust structures also were mentioned by Nullo et al. (1998) between the Salado and Grande Rivers. A backthrust system at the Atuel River (Fig. 1a) has been recognized by Kozlowski et al., (1993) and Sruoga et al., (2002) and described by Fortunatti and Dimieri (1999, 2002). The latter authors show that the backthrust system affects the Liasic cover sequence, though it could be genetically related to the uplift of basement blocks (Fortunatti et al., 2004; Turienzo et al., 2004). As we have mentioned, the Lomas Bayas structure (Fig. 4) is a basement-cored, west-vergent anticline with a slightly tilted eastern limb (10°E) and steeper western limb (35°W).

Previously, few models have been available to explain the geometric and kinematic development of backthrusts associated with major structures. Backthrust systems may have been emplaced as subordinated structures in two ways. First, they could be associated with faults that steepen upward (Fig. 6) with listric or planar geometry (Coward et al., 1991). In this case, backthrusts are generated similarly to an antithetic structure related to a bend or high curvature zone in the fault to accommodate hangingwall deformation (Dahlstrom, 1969; Serra, 1977; Coward et al., 1991; Mitra, 2002). The formation of antithetic faults by this mechanism is possible in both extensional and contractional regimes; in the latter case, the backthrust can be a new or an older normal fault reactivated in a reverse sense (Hayward and Graham, 1989). The resultant geometry would be a triangular block bound by reverse faults on both sides with an unbent roof. This geometry is known as a 'pop-up' structure (Fig. 6c). Second, Banks and Warburton (1986) propose that backthrusts may form in the upper part of a passive roof duplex. A variant of this model, adapted to a basement-driven wedge, was proposed by Dimieri (1997),

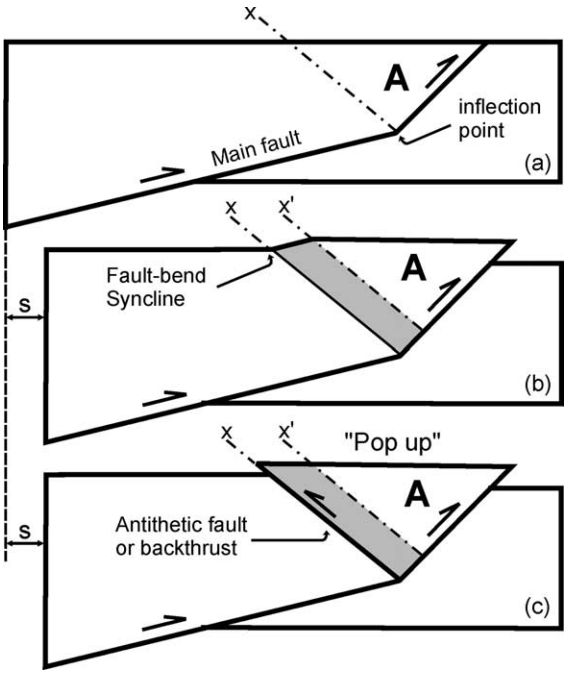

Fig. 6. Simplified model showing the hangingwall deformation related to a planar fault with dip changes or bends (adapted from Mitra, 2002). (a) Stage before deformation. (b) Folding of materials that pass through the axial surface x to accommodate the hangingwall deformation. (c) Growth of an antithetic fault (or backthrust) resolves the deformation and gives way to a pop-up structure. Area balance is not strictly conserved.

in which backthrusts form at the leading branch line of a wedge emplaced by blind thrusting. Because we interpret the main structure as a basement block uplifted by a reverse fault that reached the surface, this basement wedge model is not suitable.

We show the formation of pop-up structures in Fig. 6a, in which a triangular sector is depicted between an imaginary line (x) and the steeper dipping part of the fault. After an arbitrary shortening (s), this constant area block (A) moves from its original position. Material of the hangingwall block that passes through the x line can be deformed by folding or faulting or a combination thereof (Dahlstrom, 1969; Mitra, 2002). Straining in these rocks (shadow sectors, Fig. 6) can produce small area variations. In the first case, the resulting structure could be a fault-bend syncline (Fig. 6b), in which the x line acts as an active axial surface that does not need to bisect the interlimb angle and is trigonometrically related to the tilt of folded layers (Narr and Suppe, 1994). Alternatively, hangingwall deformation could be resolved by means of an antithetic fault. Generally, this new fault would have similar dip (moderate to high) to that of the upper part of the main fault (Fig. 6c). The latter mechanism is responsible for pop-up structures. In this case, if no other deformation mechanism acts on it, the roof of the triangular block remains in its original position, which in its simplest case is horizontal. Thus, the tilted eastern limb of the Lomas Bayas anticline cannot be explained by this basic model without extra rotation. If the antithetic structure were a reactivated normal fault, it would have a higher dip. In our model, the antithetic fault becomes horizontal when it reaches the basement–cover interface and produces a basement wedge. This folding of the toe of the basement triangular block would be difficult to accomplish with high-angle faults. For these reasons, we need an improved model, with geometrical constraints, that can be adapted to the actual structural configuration of the study area.

To describe the complete structural evolution in a detailed manner, we consider it appropriate to construct a new schematic and relatively simple kinematic model that explains backthrust development in basement rocks at shallower levels (brittle–semibrittle conditions). First, we consider a basement block limited on its left side by a vertical line placed arbitrarily at a point v (Fig. 7a) and on its

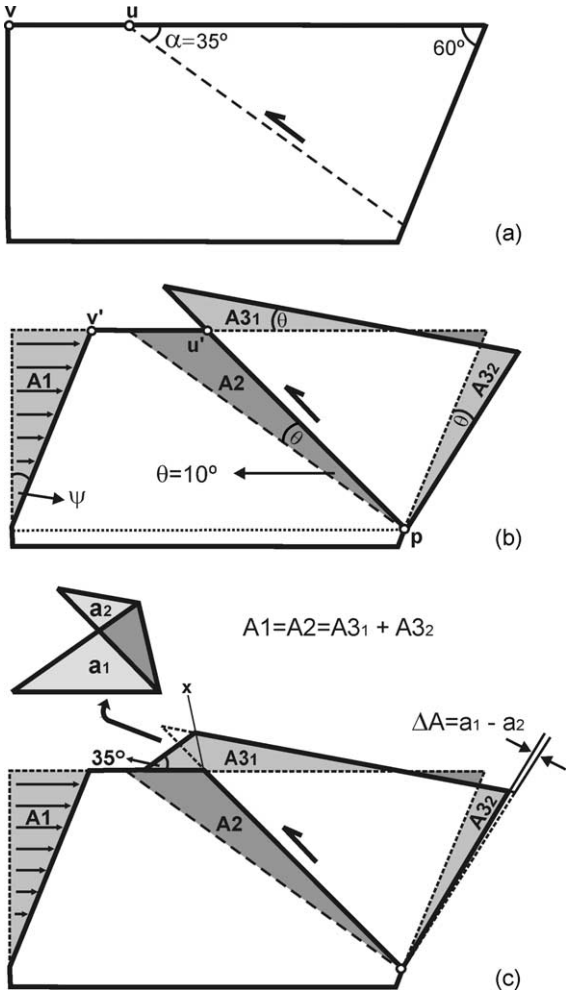

Fig. 7. Quantitative geometric and kinematic model to explain the generation of backthrusts related to uplifted basement blocks. (a) Stage before backthrust generation. Dotted line shows the backthrust initial dip ($\alpha = 35°$). (b) Basement block with triangular or wedge shape above the backthrust rotates progressively 10° (θ) around the p point due to angular shearing (ψ). Note that the deformed areas are constant. (c) The toe of the basement wedge is bent, generates a minor anticline, and delaminates the overlying sedimentary rocks. The growth of this structure implies an area excess (Δa) that can be resolved by a small wedge rotation or small-scale structures, mainly developed at the hinge zone.

right side by a 60° tilted line, which is interpreted as a moderate to steeply dipping previous fault. According to our model, this latter fault becomes inactive and begins to behave like a buttress against a push from the left. Second, a shearing builds on the left side and generates a low to moderately angled backthrust fault ($\alpha = 35°$). The basement block above the backthrust has a triangular or wedge shape, so we tilt the hangingwall block with a rotation. To produce this rotation, differential shortening, which begins at the structural level where the backthrust intersects the main fault (dotted line, Fig. 7b) and has a maximum value at the basement–cover interface, is needed. This deformation occurs through shearing from the left side of the model and thereby affects the basement rocks above the structural level, because the amount of shear is related directly to the required wedge tilt. This shearing displaces points u and v (Fig. 7a) to positions u' and v' (Fig. 7b). The vertical line on v becomes a tilted line on v' after deformation. The rotation angle ψ that the line undergoes represents shearing that affects basement rocks. The triangular block above the backthrust rotates rigidly at an angle of θ (here, 10°) around p located in the branch line between the backthrust and the main fault. As Fig. 7 shows qualitatively, in this model, there is a direct relationship between angular shear (ψ) and the wedge rotation angle (θ). According to this relationship, low shear amounts produce minor wedge tilting, and vice versa. Furthermore, we can deduce that, with constant angular shear, block rotation will be lesser with a smaller backthrust initial dip. These statements are supported by the following equation, whose graphical representation appears in Fig. 8:

$$\theta = \sin^{-1}\left(\frac{\tan\psi \sin\alpha}{\sqrt{\tan^2\psi + \operatorname{cosec}^2\alpha - 2\tan\psi\cot\alpha}}\right). \quad (1)$$

The analytical development of this function, which relates the backthrust rotation angle (θ) to its initial dip (α) and the applied angular shear (ψ), is depicted in detail in the Appendix. In the schematic model (Fig. 7b), all material lines above the backthrust rotate 10°. Thus, the backthrust initially generated with low dip (35°) finally reaches 45°. In Fig. 8, we show that a fault's final tilt ($\alpha+\theta$) can be obtained by combining different values of the fault's initial angle (α) and block rotation angle (θ). For example, consider the structure of Lomas Bayas, formed by a backthrust with a 45° final dip, which in our interpretation results from rotating 10° a fault with 35° initial dip (Fig. 8). This tilt also could result from rotating, for example, 15° or 25° a fault with 30° or 20° initial dips, respectively. Although our geometric model allows a wide rotation range, geological and physical reasons induce us to consider only small rotations. Large rotations would require large angular shears that would produce a concomitant internal strain on the basement rocks at the footwall and the buttress block to the right, which is unlikely in shallow deformation conditions.

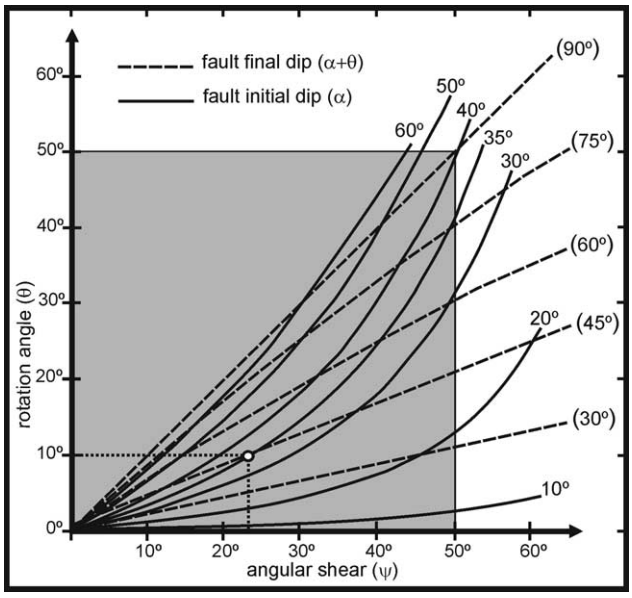

Fig. 8. Graphic representation of the equation used to calculate the backthrust rotation angle (θ) based on its initial dip (α) and applied (ψ) angular shear (see Appendix). Continuous lines represent fault initial dips, and dashed lines indicate fault dips after rotation. Note that a fault final dip can be obtained by combining different rotations and fault initial dips, but variable amounts of angular shear are required. The white circle shows the data for the Lomas Bayas structure.

The geometric model proposed here follows the rules of volume conservation; namely, there is no material loss or gain during deformation. Small-scale structures can occur to resolve slight shape changes of the basement rocks. Brittle fracture and cataclasis along discrete faults, fractures, and veins, with little or no displacement, are common mechanisms that could accommodate small amounts of deformation in shallower tectonized rigid materials (Evans et al., 1993; Wibberley, 1997). We note that the surface displaced by shearing ($A1$) is equal to the surface ($A2$) swept by the wedge from its original position (dashed line, Fig. 7b) to its deformed state. The latter area is equal to $A3_1 + A3_2$, which depart from the initial position because of wedge rotation. Therefore, to finish our schematic model that illustrates basement wedge rotation, we must add a last step. In Fig. 7b, we show the triangular sectors rotating rigidly, which means that faulting would penetrate the sedimentary cover cross-cutting upward. Thus, the toe of the backthrust-related basement block would intrude a sharp end in the overlying strata, which, despite its plausibility, is not observed in the study area. We propose that, when deformation starts, the tip of the backthrust propagates as a footwall flat that follows a detachment level, probably at the basement–cover interface, though an upper level detachment also is likely. The detachment between the basement and sedimentary units is a necessary condition for our general geometric and kinematic model, as we demonstrate subsequently. As rotation continues, the toe of the wedge reaches the basement–cover interface (or an

upper level) and delaminates the sedimentary sequence. It then begins to bend in a way that suggests a fault-bend folding mechanism (Suppe, 1983), though in this case, the forelimb dip equals the fault dip. Hangingwall material that passes through axial surface x (Fig. 7c) changes its position from horizontal to a dip equivalent to that of the backthrust, though in an opposite sense. In turn, the fold's forelimb dip should grow continuously when the backthrust becomes steeper. Then, this limb must have a variable geometry with a 35° minimum slope in its lower part and 45° maximum dips in the upper part. This progressive limb rotation would result in a curved limb. For simplicity, we assign a constant dip of 35°, in accordance with most field measurements. As we show in Fig. 7c, the bent toe area (a_1) is larger than the same area before bending (a_2). We theorize that the cutoff angle of the backthrust remains unchanged at the forelimb, unlike the fault-bend model. This area difference (Δa) could be accommodated by a similar amount of material entering from the opposite side or by a smaller rotation of the triangle base (in this case, approximately 1°30′ smaller). Furthermore, though it has not been observed in the field, small-scale structures likely develop in response to the internal strain of the wedge and contribute at least partially to compensate for this area difference. These small-scale structures, faults, or fractures should develop mainly in the anticline hinge zone. In most models of thrust sheet deformation, these structures develop due to shearing on steep planes or zones above a bend (Fischer and Coward, 1982; Knipe, 1985). In an isotropic medium, such as basement rocks moving over a ramp-flat bend, the shear strain is minimal when the shear plane bisects the ramp-flat angle (Wibberley, 1997). We do not consider this slight area variation in our general geometric and kinematic model because its effects at a regional scale should be insignificant.

5. General geometric and kinematic model

To explain the structural characteristics of the study area, we adapt the schematic model to a large-scale model. We mentioned previously that an important geological feature in the Diamante River area is the thinning of the cover layers above the eastern edge of the basement block, which was uplifted by the Carrizalito fault. This strata thinning is observed only in the steeper limb of this huge structure and therefore suggests a tectonic origin (Fig. 5). Furthermore, small-scale extensional faults appear in these thinned rocks. Another important feature is the difference in the basement elevation in the sides of the Carrizalito fault (Baldi et al., 1984). These geological characteristics are essential for choosing a kinematic model for the region. Several works depict regional cross-sections that show basement-involved structures, but only a few show their detailed geometry or analyze their kinematic evolution. Most models that imply basement-involved structures have several similarities; in particular, almost all models based on moderate- or high-angle faults show great altitude differences among faulted blocks and an important thinning and stretching of the cover strata (e.g. Erslev, 1991; Erslev and Rogers, 1993; McConnell and Wilson, 1993; Evans et al., 1993; Narr and Suppe, 1994; Allmendinger, 1998; Mitra and Mount, 1998). We follow the techniques proposed by Narr and Suppe (1994) to explain the development of the Cordón del Carrizalito structure. Their model is based on the geometric relationships and kinematic history of the elements that form a fault–fault–fold triple junction and has been applied to the confluence of the Atuel River with the Blanco stream, which presents a complex structural evolution of basement and cover rocks (Turienzo et al., 2004). Although this model is appropriate to explain the bulk geometry of the faulted blocks, it does not account for the related small-scale structures. Therefore, we analyzed the development of the Lomas Bayas structure through the basement-involved backthrust model proposed herein. Moreover, by combining this model with that of Narr and Suppe (1994), we obtain a final geometry that fits the field data reasonably well.

In Fig. 9a, we show sedimentary cover layers above a basement block in an undeformed state. Within the basement block, we show elements of a fault–fault–fold triple junction. A west-dipping fault with a moderate to high angle ($\theta = 60°$) joins a previous vertical fault ($\varepsilon = 90°$), which could be the upper part of a listric fault. The vertical fault is not visible in the field and thus represents an interpretation that enables us to apply the triple junction model. The model explanation is focused on the deformation of the frontal structure, though the main fault could decrease its dip downward. The third element of the triple junction is an axial surface with a dip of 30° (ϕ). Basement rocks placed between this axial surface and the vertical fault could undergo penetrative, uniform shear (Narr and Suppe, 1994). The upper part of this triangular sector tilts 30° when the main fault reaches the basement–cover interface (Fig. 9b). Because of the deformation of the basement rocks, the length of the basement compared with the cover changes at the interface, which generates a detachment between the structural units that results in differential shortening (Cs_1) at the eastern edge of the cross-section.

Conversely, if the interface is not detached, extensional structures in the sedimentary sequence could explain the slight length difference (Turienzo et al., 2004). At this stage, the lower fault passively displaces the vertical fault, while a drape fold forms in the cover beds. With greater orogenic contraction, the hangingwall block protrudes the sedimentary cover, produces an important thinning and stretching of the layers, and overturns them below the main fault (Fig. 9c). In a later stage, as deformation continues, the Carrizalito fault breaks through the thinned beds and displaces the hangingwall block without affecting the footwall rocks (Fig. 9d). The final height difference among the basement-faulted blocks takes place in this stage. Somehow, the displacement of the main fault slows,

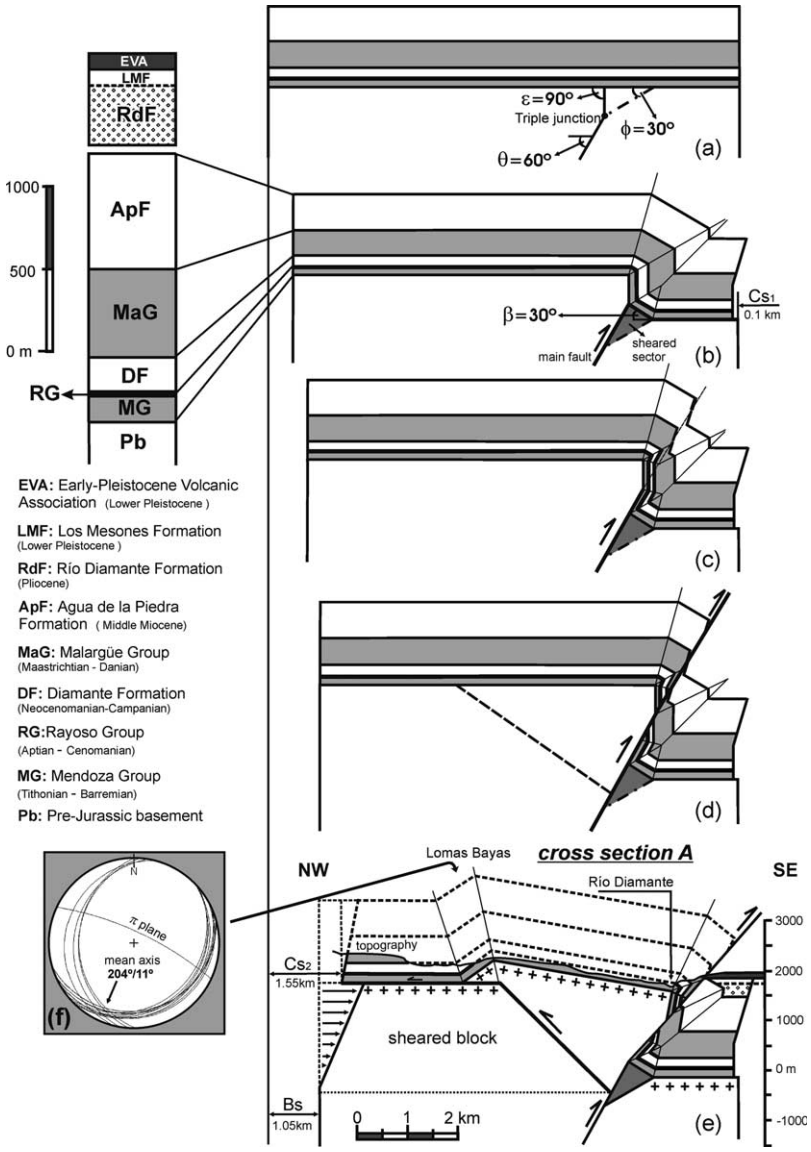

Fig. 9. Geometric and kinematic model that explains the structural evolution in the study area. The reconstructions at stages a–d are based on the model of basement-involved compressive structures by Narr and Suppe (1994); that for stage e uses the new kinematic model developed herein (see Fig. 7). (a) Stage before deformation showing the elements of the fault–fault–fold triple junction within a basement block. (b) Development of a drape fold in the sedimentary cover. The shearing of the basement rocks changes the length of the basement–cover contact, which can be resolved by the detachment and differential shortening Cs_1 between the structural units. (c) The hangingwall block protrudes into the sedimentary section and causes layer thinning and stretching ahead of the fault, while beds below the fault are overturned. (d) The fault cuts the cover rocks, and the hangingwall is displaced toward the foreland. (e) Shearing on basement rocks generates the backthrust and related anticline structure, which represents the final configuration for cross-section A and shows the attained shortening. (f) Axis orientation of the Lomas Bayas anticline calculated by plotting field data from both limbs in a Schmidt-Lambert equal area stereographic net.

maybe due to huge molasses accumulations at the mountain front that obstruct forward movement. Finally, a backthrust develops to form the Lomas Bayas fold (Fig. 9e). As we stated previously, this backthrust is generated in response to the shearing of basement rocks, which may be due to pushing from the west produced by out-of-sequence thrust systems and folding, with respect to the Carrizalito fault, that progresses at the upper levels of the basement rocks. Such out-of-sequence thrust systems have been reported in several regions of the Cordillera Principal (Giambiagi and Ramos, 2002). Moreover, these basement rocks could have borne shearing, due to their heterogeneity in most areas (low-grade metamorphic rocks, volcaniclastic and intrusive sequences). This deformation then rotates the basement above the backthrust. The toe of this sector is bent and therefore delaminates the sedimentary cover that acts as a wedge. Layers of the main fault footwall are deformed by the wedge rotation, as shown in a simplified manner in Fig. 9e. The figure also depicts the final stage of cross-section A (location in Fig. 1b) and is a modeled configuration that corresponds reasonably well with the attitude of the field structures.

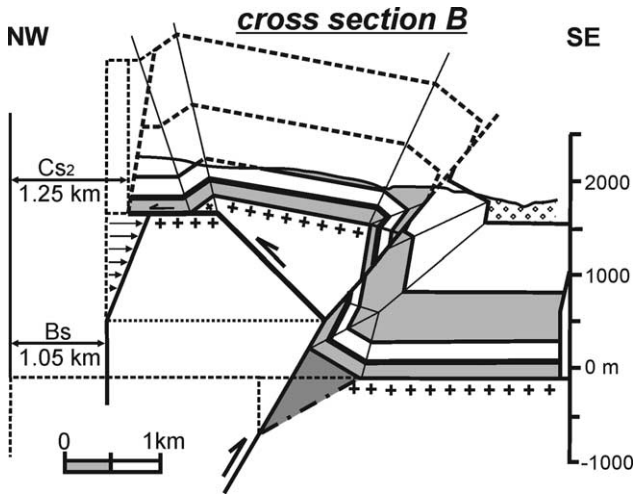

Fig. 10. Interpreted structural configuration and shortening calculated for cross-section B. The kinematic evolution is similar to that of cross-section A (see Fig. 9 for references).

Retrodeformable models applied to different cross-sections enable us to calculate the shortening. Basement shortening was calculated without considering the backthrust development. In cross-sections A (Fig. 9e) and B (Fig. 10), both basement-shortening values are 1.05 km. Along cross-section B, younger stratigraphic units outcrop (Fig. 1b), which may indicate a southwestern plunge of the structures. According to our interpretation, the reconstructions in both cross-sections have the same kinematic history until the stage before backthrust development (Fig. 9a–d). Therefore, the structure related to the Carrizalito fault reaches the same structural level, as is supported by the similar basement-shortening values and the fact that, in both sections, the hangingwall basement–cover interface reaches the same topographic level. The backthrust and its related anticline become attenuated to the south and probably completely disappear farther south. This feature appears in cross-section B, where the backthrust branches from the main fault at a higher point and thereby affects a smaller basement block (Fig. 10) and produces an anticline with lesser amplitude than does cross-section A.

An opposite situation occurs north of the Diamante River, where a long limb that dips a few degrees to the southeast (Figs. 1b and 3) could be correlated with the eastern limb of the Lomas Bayas anticline. If we consider that, in both cross-sections, the Carrizalito fault uplifts the basement blocks to the same topographic level (Fig. 9d), a southward-plunging axis could be accountable for the attenuation of the backthrust-related anticline. From the cross-sections and orthographic methods, we calculate that the axis of the Lomas Bayas anticline plunges approximately 10° SSW. This value is in agreement with field data that, treated with a Schmidt-Lambert equal area stereographic net, suggest an 11°-plunging axis (Fig. 9f). The shortening of the sedimentary cover has been calculated at the Mendoza Group level, which can be used as a key bed in the study area. The calculated values represent a minimum shortening for the Mesozoic layers, because the bed-parallel shearing that affects the sedimentary sequence at the northwest end of both cross-sections was not considered (Figs. 9e and 10). This bed-parallel shearing, which increases upward, is required for the modeled fold geometry of the Lomas Bayas structure. Cover rock shortening (Cs_2), due to the large basement-involved structure and the backthrust-related anticline, is 1.55 km in cross-section A (Fig. 9e) and 1.25 km in cross-section B (Fig. 10). To obtain the bulk shortening of the Mesozoic beds, we must add the basement–cover differential shortening (Cs_1), which has been calculated as 0.1 km for both cross-sections.

6. Discussion

The proposed model to explain the structure of Cordón del Carrizalito consists essentially of a large basement block moving rigidly eastward by means of a high-angle reverse fault. The transported structure overthrusts Mesozoic and older rocks above Tertiary molassic sediments. This interpretation agrees with previous works performed in this region (Groeber, 1938; Polanski, 1958).

The upper part of the Carrizalito fault joins with a previous vertical fault that forms part of the eastern edge of a basement hangingwall block. According to our model, this block is rigidly uplifted and only slight bends are possible, as has been interpreted for nearby localities of the Malargüe fold-and-thrust belt (Turienzo et al., 2004). In addition, the model predicts slight rotations and gentle folding of the basement-involved structures with minor internal strain, which is significantly different from models that interpret a folded basement as major asymmetric anticlines with overturned limbs (Kozloswki, 1984; Kozlowski et al., 1993; Manceda and Figueroa, 1995).

The lack of outcropping rocks of the Cordillera Frontal to the south of the studied area has been postulated as due to the loss of slip of the Carrizalito fault (Kozloswki et al., 1989) or a normal displacement of the Las Aucas fault (Nullo and Stephens, 1993). Nevertheless, there is no field evidence of normal faulting (Ramos, 2002), and our two interpreted cross-sections show that, at least locally, there is no slip difference in the main fault. However, for larger distances, slip probably decreases southward along the fault and is accountable for the Cordillera Frontal regional plunging.

The Lomas Bayas structure is interpreted as a west-vergent anticline related to a backthrust that branches at the eastern edge of an uplifted basement block. Thus, a basement wedge forms above the backthrust, and its toe bends while the sedimentary cover is delaminated and detached from the basement. This backthrust could correspond to some of the antithetic faults that branch from the Carrizalito fault, as proposed by Nullo and

Stephens (1993), but these authors suggest the Lomas Bayas anticline formed by the accommodation of sedimentary strata above basement-driven subvertical dip-slip faults. Also, the anticline has been associated with an east-dipping fault (Kozlowski et al., 1993) that develops above a major structure in which both basement and cover deform without detachment because plastic levels are lacking (Kozloswki, 1984). A detachment between the Mesozoic layers and the basement is a feature of our model that can explain the differential shortening of these units, in contrast to those models without detached levels in which the sedimentary sequence and basement act together and thus both bear the same shortening (Kozloswki, 1984; Baldi et al., 1984).

In our view, the plunge of the Lomas Bayas anticline a few degrees south relates to the attenuation of this structure, not to a regional plunge of the basement. In our model, the Lomas Bayas anticline is the last developed structure, so it should fold previous structures such as the El Sosneado thrust (Fig. 1b).

Radiometric data about faulting-related volcanic bodies indicate that the Carrizalito fault started to develop approximately 5 Ma ago (Nullo and Stephens, 1993), though it is not known when it stopped. Farther north, the Cordillera Frontal uplift took place before 3.4 Ma (Giambiagi and Ramos, 2002). The influence of neotectonic movements on Quaternary volcanic and sedimentary rocks has been highlighted by Polanski (1962, 1963). At the Diamante River, a basaltic flow, approximately 2 Ma old and assigned to the Early Pleistocene volcanic association, is bent (Fig. 3). This feature could have originated with Quaternary activity of preexistent faults (Kozloswki, 1984). To the west, a subhorizontal lava flow lies unconformably on folded Mesozoic layers. Thus, basaltic flow flexure is not related to Mesozoic or Cenozoic deformation, which took place before 2 Ma. According to these criteria, the deformation of volcanic materials should be considered a consequence of modern movements with slight slip. Moreover, older fault reactivation could produce a fault scarp, and thus, the basaltic lava flow would have adapted to this geomorphic feature.

In our model, the structures that affect the sedimentary cover are directly related to basement deformation. This genetic link between the deep basement structure and cover deformation accords with the idea that the Cordillera Frontal and Cordillera Principal deformed simultaneously due to a system of thick-skinned, basement-driven, Cenozoic faulting, as stated by Polanski (1962, 1963).

7. Conclusion

We develop a retrodeformable, geometric, and kinematic model to explain accurately the major and minor structures that outcrop at the Las Aucas stream and Diamante River. It represents a combination of a well-known model for the basement-involved structures and a new kinematic model to explain related smaller structures.

The huge Cordón del Carrizalito structure is interpreted as a rigid basement block bound on the east by a high-angle reverse fault that produced intense deformation in the sedimentary cover. An important offset between the faulted basement blocks caused the thinning and stretching of the overlying beds, which finally were cut and displaced by the main fault. The Lomas Bayas structure thus represents a backthrust-related, west-vergent minor anticline.

In the new kinematic model proposed to explain the backthrust structural evolution, a triangular or wedge-shaped basement block, formed above the backthrust, progressively rotates due to shearing on the underlying rocks. When the toe of the wedge begins to tilt, it folds with a forelimb dip similar to that of the backthrust and thus delaminates the sedimentary sequence.

A quantitative analysis of this model indicates that the angular shear is directly related to the wedge rotation angle. Furthermore, given a fixed rotation, the required angular shear will be larger if the backthrusts have smaller initial dips.

The basement shortening that produced the large hangingwall uplift was calculated for two retrodeformable cross-sections (1.05 km for both profiles). The total cover shortening varies from 1.65 km in cross-section A to 1.35 km in cross-section B.

The southward attenuation of the backthrust-related anticline explains the outcropping of younger stratigraphic units in this sector.

The uplift and deformation of the Cordillera Frontal's southern border by the Carrizalito fault is linked intimately with the deformation of Cenozoic and Mesozoic rocks of the Cordillera Principal. Furthermore, we believe this structural relationship was generated by a system of thick-skinned, basement-driven faults during the Andean orogeny.

Acknowledgements

The authors acknowledge financial support from the Geology Department and SeCyT of the Universidad Nacional del Sur and CONICET. They thank Sergio Delpino for a thorough review and Sebastian Ferraro for his helpful collaboration on trigonometric analysis. Many thanks also are due to Natalia Fortunatti and Celeste Bolognani for their assistance in the field. The authors are grateful for the reviews of Ernesto Cristallini and Tomas Zapata, which considerably improved the article.

Appendix A

We propose a schematic kinematic model to explain the Lomas Bayas anticline by the rotation of a backthrust-related basement wedge. We have mentioned the geological

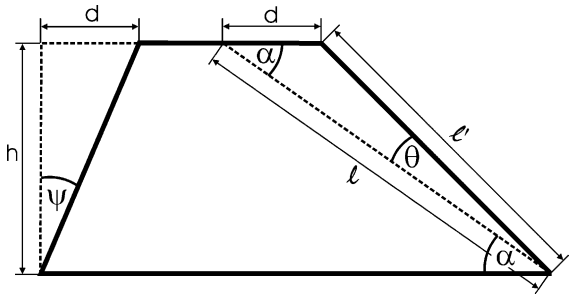

Fig. A1.

processes needed to obtain such a deformation and qualitatively described the geometric relationships among the involved parameters. Here, we develop an area-constant quantitative model. We first consider a quadrilateral (Fig. A1) that, in an initial stage, has an arbitrary height (h). A line whose inclination is α and length is l forms the quadrilateral's left side and represents the backthrust. When shearing is applied, the body deforms but maintains its constant height h, which implies no area loss. This constraint ensures that the geometric model is balanced. Using this quantitative model, we can calculate the backthrust (or wedge) rotation (θ) related to the angular shear (ψ) applied to the right side of the quadrilateral. As in Fig. A1, the slip (d) that affects both sides of the quadrilateral is equal. Thus, the relationship between the rotation angle and the shear angle is constrained by the initial position of the lines, in this case, the initial fault dip (α).

According to the sine rule, we find

$$\frac{\sin\theta}{d} = \frac{\sin\alpha}{\ell'}, \tag{A1}$$

and

$$\theta = \sin^{-1}\left(d\frac{\sin\alpha}{\ell'}\right). \tag{A2}$$

In Fig. A1, slip (d) is directly related to angular shear (ψ) by

$$d = h\tan\psi, \tag{A3}$$

and following the cosine rule, we find that

$$\ell'^2 = d^2 + \ell^2 - 2d\ell\cos\alpha, \tag{A4}$$

and

$$\ell' = \sqrt{d^2 + \ell^2 - 2d\ell\cos\alpha}. \tag{A5}$$

Therefore, knowing the relationship

$$\ell = \frac{h}{\sin\alpha}, \tag{A6}$$

we can insert Eqs. (A3) and (A6) into Eq. (A5) to obtain the length ℓ' as a function of the angles α and ψ and one-dimensional parameter h, as follows

$$\ell' = \sqrt{(h\tan\psi)^2 + \left(\frac{h}{\sin\alpha}\right)^2 - 2h\tan\psi\frac{h}{\sin\alpha}\cos\alpha}, \tag{A7}$$

which is equal to

$$\ell' = h\sqrt{\tan^2\psi + \frac{1}{\sin^2\alpha} - 2\frac{\tan\psi}{\tan\alpha}}. \tag{A8}$$

Finally, substituting Eqs. (A3) and (A8) into Eq. (A2), we achieve the function that expresses the backthrust rotation angle (θ) related to its initial dip (α) and the angular shear (ψ)

$$\theta = \sin^{-1}\left(\frac{\tan\psi\sin\alpha}{\sqrt{\tan^2\psi + \frac{1}{\sin^2\alpha} - 2\frac{\tan\psi}{\tan\alpha}}}\right), \tag{A9}$$

which is the same as

$$\theta = \sin^{-1}\left(\frac{\tan\psi\sin\alpha}{\sqrt{\tan^2\psi + \operatorname{cosec}^2\alpha - 2\tan\psi\cot\alpha}}\right). \tag{A10}$$

As these equations demonstrate, angular variations among different parameters are size independent. Therefore, we develop an equation that provides different geometric relationships using only angular data. We draw the curve that corresponds to this function for some initial dip values (Fig. 8), in which the variations between the mentioned parameters are evident. With this set of curves, we can easily quantify the angular shear needed to produce rotations from different initial fault dips.

References

Allmendinger, R., 1998. Inverse and forward numerical modeling of trishear fault-propagation folds. Tectonics 17 (4), 640–656.

Baldi, J., Ferrante, R., Ferrante, V., Martinez, R., 1984. Estructuras de bloques y su importancia petrolera en el ámbito Mendocino de la cuenca Neuquina, IX Congreso Geológico Argentino, Actas 4, Buenos Aires, pp. 153–161.

Banks, W., Warburton, J., 1986. 'Passive-roof' duplex geometry in the frontal structures of the Kirthar and Sulaiman mountain belts, Pakistan. Journal of Structural Geology 8, 229–237.

Bettini, F., Pombo, R., Mombru, C., Uliana, M., 1978. Consideraciones sobre el diastrofismo andino en la vertiente oriental de la Cordillera Principal, entre los 34°30′ y los 37° de latitud sur, VII Congreso Geológico Argentino, Actas 1, Buenos Aires, pp. 671–683.

Combina, A., Nullo, F., Stephens, G., 1993. Depósitos Terciarios en el pié de sierra del área de Las Aucas, sur de Mendoza, XII Congreso Geológico Argentino y II Congreso de Exploración de Hidrocarburos, Actas 2, Mendoza, pp. 180–186.

Combina, A., Nullo, F., Stephens, G., Baldauf, P., 1994. Paleoambientes de la Formación Agua de la Piedra, Mendoza, Argentina, VII Congreso Geológico Chileno, Actas 1, Santiago, pp. 418–424.

Coward, M., Gillcrist, R., Trudgill, B., 1991. Extensional structures and their tectonic inversion in the Western Alps. In: Roberts, A., Yielding, G., Freeman, B. (Eds.), The Geometry of Normal Faults. Geological Society, Special Publication 56, , pp. 93–112.

Cruz, C., 1993. Facies y estratigrafía secuencial del Cretácico superior en la zona del río Diamante, Provincia de Mendoza, Argentina, XII Congreso

Geológico Argentino y II Congreso de Exploración de Hidrocarburos, Actas 1, Mendoza, pp. 46–54.

Dahlstrom, C., 1969. Balanced cross-sections. Canadian Journal of Earth Sciences 6, 746. In: Thrust-Faulted Terranes, American Association of Petroleum Geologists reprinted series 27, pp. 57–71.

Dimieri, L., 1992. Evolución estructural de la Cordillera Principal, a lo largo del Ao. La Vaina, entre el Potimalal y el Pehuenche, al oeste de Bardas Blancas, Mendoza. Biblioteca Central, Universidad Nacional del Sur, Thesis, Bahía Blanca, 156 p.

Dimieri, L., 1997. Tectonic wedge geometry at Bardas Blancas, Southern Andes (36°S), Argentina. Journal of Structural Geology 19 (11), 1419–1422.

Dimieri, L., Nullo, F., 1993. Estructura del frente montañoso de la Cordillera Principal (36° latitud sur), Mendoza, XII Congreso Geológico Argentino y II Congreso de Exploración de Hidrocarburos, Actas 3, Mendoza, pp. 160–167.

Erslev, E., 1991. Trishear fault-propagation folding. Geology 19, 618–620.

Erslev, E., Rogers, J., 1993. Basement–cover geometry of Laramide fault-propagation folds. In: Schmidt, C.J., Chase, R.B., Erslev, E.A. (Eds.), Laramide Basement Deformation in the Rocky Mountain Foreland of the Western United States. Geological Society of America Special Paper 280, Boulder, CO, pp. 125–146.

Evans, J., DuBois, M., Batatian, D., Derr, D., Douglas, N., Harlan, S., Malizzi, L., McDowell, R., Nelson, G., Parke, M., Schimdt, C., Weberg, E., 1993. Deformation mechanisms and kinematics of a Precambrian-cored fold and fault structure: Jakeys Fork structure, notheastern Wind River Range, Wyoming. In: Schmidt, C.J., Chase, R.B., Erslev, E.A. (Eds.), Laramide Basement Deformation in the Rocky Mountain Foreland of the Western United States. Geological Society of America Special Paper 280, Boulder, CO, pp. 163–176.

Fischer, M., Coward, M., 1982. Strains and folds within thrust sheets: an analysis of the Heilam sheet, northwest Scotland. Tectonophysics 88, 291–312.

Fortunatti, N., Dimieri, L., 1999. Reconstrucción estructural del perfil del valle del río Atuel. Grupo Cuyo. Mendoza, XIV Congreso Geológico Argentino, Actas 1, Salta, pp. 224–226.

Fortunatti, N., Dimieri, L., 2002. Zonación Estructural entre los arroyos Blanco y Malo en el área del río Atuel, Mendoza, Argentina, XV Congreso Geológico Argentino, Actas 3, El Calafate, pp. 206–213.

Fortunatti, N., Turienzo, M., Dimieri, L., 2004. Retrocorrimientos asociados al frente de avance orogénico, arroyo Blanco, Mendoza, Asociación Geológica Argentina, Serie D: Special Publication. 7, 34–40.

Giambiagi, L., Ramos, V., 2002. Structural evolution of the Andes in a transitional zone between flat and normal subduction (33°30′–33°5′S) Argentina and Chile. Journal of South American Earth Sciences 15, 101–116.

Giambiagi, L., Tunik, M., Ghiglione, M., 2001. Cenozoic tectonic evolution of the Alto Tunuyán forelan basin above the transition zone between the flat and normal subduction segment (33°30′–34°S), western Argentina. Journal of South American Earth Sciences 14, 707–724.

Ghert, E., 1931. La estructura geológica de la Cordillera Argentina entre el río Grande y el río Diamante en el sud de la provincia de Mendoza, Actas Academia Nacional de Ciencias República Argentina 10, Córdoba pp. 123–174.

Gorroño, R., Nakayama, C., Viller, D., 1984. Evolución estructural del pié de sierra externo en la zona de Malargüe, Provincia de Mendoza, IX Congreso Geológico Argentino, Actas 2, Buenos Aires, pp. 125–136.

Groeber, P., 1938. Mineralogía y Geología,. Espasa-Calpe Argentina, Buenos Aires.

Observaciones geológicas a lo largo del meridiano 70, Pt. 1: Hoja Chos Malal. Revista de la Asociación Geológica Argentina 1, 177–208. Reprinted in Asociación Geológica Argentina, Serie C 1, 1–174 (1980).

Observaciones geológicas a lo largo del meridiano70, Pt. 2: Hojas Sosneao y Maipo. Revista de la Asociación Geológica Argentina 2 (2), 141–176 (Reprinted in Asociación Geológica Argentina, Serie C1, 1–174 (1980).

Hayward, A., Graham, R., 1989. Some geometrical characteristics of inversion. In: Cooper, M., Williams, G. (Eds.), Inversion Tectonics. Geological Society Special Publication Classics, Londres, pp. 17–39.

Knipe, R., 1985. Footwall geometry and the rheology of thrust sheets. Journal of Structural Geology 7 (1), 1–10.

Kozloswki, E., 1984. Interpretación estructural de la Cuchilla de la Tristeza. Provincia de Mendoza, IX Congreso Geológico Argentino, Actas 2, Buenos Aires, pp. 381–395.

Kozloswki, E., Baldi, J., 1983. Estratigrafía, estructura y posibilidads petroleras de la zona del Río Diamante-Río Atuel. Informe inédito YPF.

Kozloswki, E., Cruz, C., Condal, P., Manceda, R., 1989. Interpretación del fallamiento de bajo ángulo en los sedimentos cretácicos del río Diamante. Pcia. de Mendoza, I Congreso Nacional de Exploración de Hidrocarburos, Actas 2, Buenos Aires, pp. 675–688.

Kozlowski, E., Manceda, R., Ramos, V., 1993. Estructura. In: Ramos, V.A. (Ed.), Geología y Recursos Naturales de Mendoza XII Congreso Geológico Argentino y II Congreso Nacional de Exploración de Hidrocarburos. Relatorio 1 (18), pp. 235–256.

Lahee, F., 1927. The petroliferous belt in Central Western Mendoza, Argentina, American Association of Petroleum Geologists, Tulsa, OK p. 261.

Legarreta, L., Gulisano, C., 1989. Análisis Estratigráfico Secuencial de la Cuenca Neuquina (Triásico superior-Terciario inferior), Cuencas Sedimentarias Argentinas, pp. 221–243.

Llambias, E., Kleiman, J., Salvarredi, J., 1993. El Magmatismo Gondwánico. In: Ramos, V. (Ed.), Geología y Recursos Naturales de Mendoza, Relatorio 1 (6), 53-64.

Manceda, R., Figueroa, D., 1995. In: Tankard, A.J., Suárez, R.S., Welsink, H.J. (Eds.), Inversion of the Mesozoic Neuquén rift in the Malargüe fold and thrust belt, Mendoza, Argentina. Petroleum Basins of South America, AAPG Memoir 62, , pp. 369–382.

McConnell, D., Wilson, T., 1993. Linkage between deformation of basement rocks and sedimentary rocks in basement-involved foreland folds. In: Schmidt, C.J., Chase, R.B., Erslev, E.A. (Eds.), Laramide Basement Deformation in the Rocky Mountain Foreland of the Western United States. Geological Society of America Special Paper 280, Boulder, CO, pp. 319–333.

Mitra, S., 2002. Fold-accommodation faults. American Association of Petroleum Geologists Bulletin42002;, 671–693.

Mitra, S., Mount, V., 1998. Foreland basement-involved structures. American Association of Petroleum Geologists 82 (1), 70–109.

Narr, W., Suppe, J., 1994. Kinematics of basement-involved compressive structures. American Journal of Science 294, 802–860.

Nullo, F., Stephens, G., 1993. Estructura y deformación terciaria en el área de las Aucas, sur de Mendoza, XII Congreso Geológico Argentino y II Congreso de Exploración de Hidrocarburos, Actas 3, Mendoza, pp. 107–112.

Nullo, F., Proserpio, C., Haller, M., 1987. Estructuras Intercretácicas en la Cordillera Principal (34°30′-36°) Mendoza, Argentina, X Congreso Geológico Argentino, Actas 1, pp. 185–188.

Polanski, J., 1958. El bloque varísico de la Cordillera Frontal de Mendoza. Asociación Geológica Argentina, Revista 12 (3), 165–196.

Polanski, J., 1962. Interpretación tectónica de la geomorfología del borde oriental de la Cordillera Frontal de Mendoza, Anales I Jornadas Geológicas Argentinas, Actas 2, Buenos Aires pp. 245–256.

Polanski, J., 1963. Estratigrafía, Neotectónica y Geomorfología del Pleistoceno pedemontano de Mendoza. Asociación Geológica Argentina, Revista 17 (3–4), 181–199.

Ramos, V., 2002. La transición entre las Fajas Plegadas y Corridas de Aconcagua y Malargüe: Influencia del basamento de la Cordillera

Frontal, XV Congreso Geológico Argentino, (Comunicación), Actas 3, El Calafate, pp. 166–167.

Serra, S., 1977. Styles of deformation in the ramps regions of overthrusts faults. Wyoming Geological Association Handbook, XXIX Annual Field Conference, pp. 487–498.

Sruoga, P., Etcheverría, M., Folguera, A., Repol, D., 2002. Hoja Geológica 3569-I, Volcán Maipo, Provincia de Mendoza, SEGEMAR, Boletín 290 pp. 1–114.

Suppe, J., 1983. Geometry and kinematics of fault-bend folding. American Journal of Science 283, 684–721.

Turienzo, M., Fortunatti, N., Dimieri, L., 2004. Configuración estructural del basamento en la confluencia del arroyo Blanco y el río Atuel, Mendoza. Asociación Geológica Argentina, Serie D: Special Publication 7, pp. 27–33.

Volkheimer, W., 1978. Descripción geológica de la hoja 27b, cerro Sosneado, Provincia de Mendoza, Servicio Geológico Nacional, Boletín 151 pp. 1–85.

Wibberley, C., 1997. Three-dimensional geometry, strain rates and basement deformation mechanisms of thrust-bend folding. Journal of Structural Geology 19 (3–4), 535–550.